

ORIGINAL ARTICLE

Morphology analysis of *Escherichia coli* treated with nonthermal plasma

J. Guo^{1,2}, Z. Li¹, K. Huang¹, Y. Li^{1,3} and J. Wang¹

1 College of Biosystems Engineering and Food Science, Zhejiang University, Hangzhou, China

2 Institute of Food Science, Zhejiang Academy of Agricultural Sciences, Hangzhou, China

3 Department of Biological and Agricultural Engineering, University of Arkansas, Fayetteville, AR, USA

Keywordsdisinfection, *Escherichia coli*, food safety, nonthermal processes, sterilization.**Correspondence**

Jianping Wang, College of Biosystems Engineering and Food Science, Zhejiang University, 886 Yuhangtang Road, Hangzhou 310058, China.

E-mail: jpwang@zju.edu.cn

2016/1776: received 14 August 2016, revised 18 October 2016 and accepted 24 October 2016

doi:10.1111/jam.13335

Abstract

Aims: Nonthermal plasma agents (reactive species and charged particles) are generally generated together. Previous studies of nonthermal plasma agents did not investigate the role of a microbial inactivation agent without interference from other agents. Consequently, the exact mechanism underlying their activity remains unclear. The present experiment was conducted to study the mechanism underlying *Escherichia coli* inactivation by nonthermal plasma.

Methods and Results: The mechanism underlying *E. coli* inactivation by charged particles was studied using pure argon plasma. Results showed that cell wall damage owing to strong electrostatic forces did not occur during direct current (DC) plasma treatment with Ar or N₂. Next, the inactivation effects of excited N₂^{*}, N₂⁺, ozone, OH radicals, and nitric oxide were investigated using pure nitrogen plasma and air plasma. Morphological changes and cell rupture of *E. coli* were observed after 5 min of treatment with nonthermal plasma in air, but not with argon and nitrogen plasma treatments.

Conclusions: Our data demonstrate that reactive oxygen species play an essential role in the inactivation of *E. coli*.

Significance and Impact of the Study: A clear understanding of the mechanisms underlying nonthermal plasma's inactivation of micro-organism is essential for the practical applications of nonthermal plasma techniques.

Introduction

Atmospheric pressure nonthermal plasma (APNTP) is an innovative technology that has been studied in several fields, such as decontamination of fresh produce, microbial inactivation and food in-package decontamination (Baier *et al.* 2013; Bermudez-Aguirre *et al.* 2013; Fernandez *et al.* 2013; Jahid *et al.* 2014; Misra *et al.* 2014; Pan-kaj *et al.* 2014; Lacombe *et al.* 2015). Given its attractive features, such as low-temperature properties and high efficiency of microbial inactivation, nonthermal plasma is a promising technology for applications in many fields (Suhem *et al.* 2013; Jahid *et al.* 2015; Lee *et al.* 2015; Ziuzina *et al.* 2015; Pradeep and Chulkyoon 2016).

APNTP is composed of plasma, including UV radiation, reactive species and charged particles, at near-room temperature. Plasma is highly energetic and expected to

interact with and cause death of micro-organisms. Despite the potential uses of nonthermal plasma, the exact mechanism underlying its activity remains unclear. In fact, there is wide discrepancy in the field regarding the effects of various plasma on micro-organisms. Mendis *et al.* (2000) proposed a mechanism underlying the inactivation of bacteria by charged particles. They proposed that electrostatic forces caused by accumulation of charges on the outer surface of bacterial membranes can overcome the tensile strength of the membrane, thereby leading to rupture. This effect is observed in Gram-negative bacteria because their membrane possesses an irregular surface (Mendis *et al.* 2000). Furthermore, Mendis *et al.* (2000) pointed out that the cellular morphological changes, which had been experimentally observed by Laroussi *et al.* (1999), supported this hypothesis (Laroussi *et al.* 1999). However, some studies have reported results

that do not support this hypothesis (Deng *et al.* 2006; Fletcher *et al.* 2007; Pompl *et al.* 2009; Li *et al.* 2013). Digel *et al.* (2005) proposed an alternate model in which chemical modification of the surface proteins in bacteria was the mechanism underlying the antimicrobial action of charged particles. Specifically, in situ hydroxyl radical formation on the bacterial surface was proposed to be the primary mechanism underlying protein damage caused by charged particles (Digel *et al.* 2005).

Further development and use of plasma in food decontamination require a comprehensive understanding of the role of plasma and the mechanism underlying their interaction with micro-organisms. In this study, *Escherichia coli* was used to investigate the underlying mechanism of the interaction between charged particles and bacteria as proposed by Mendis *et al.* (2000). A plasma experimental device that used two working gases to generate APNTP was developed and used to differentiate the roles of reactive species and charged particles in bacterial inactivation.

Materials and methods

Plasma treatment system

The main experimental setup is shown in Fig. 1a. The setup consists of a plasma experimental device, optical emission spectra collection system and electrical parameter collection system. The plasma experimental device

consisted of a plasma jet and high-voltage DC power source. The plasma jet consisted of electrodes and a dielectric. A copper cylinder with an external diameter of 18 mm and thickness of 3 mm was connected to the ground as the cathode. A metal rod made of tungsten alloy with a diameter of 2 mm was connected to the high-voltage DC power source as the anode. The plasma region was at the end of the inner anode. The distance between the two electrodes was approx. 1.5 mm. The diameter of the nozzle was approx. 5 mm. To generate plasma, air or argon was used as the working gas and injected into the plasma jet. The high-voltage DC power source was capable of providing tunable output voltage. The electrical parameter collection system consisted of a digital oscilloscope, current probe and high-voltage probe. A digital oscilloscope (TDS1002B-SC; Tektronix, Inc., Beaverton, OR) equipped with a high-voltage probe (P6015A; Tektronix, Inc.) and current probe (P6021; Tektronix, Inc.) was used to monitor the applied voltage and current of the plasma jet. The working gas flow rate was monitored using a rotameter. The temperature of the plasma was measured with a handheld noncontact thermometer (RAYST60; Raytek, Beijing, China) when the plasma jet was operated. The optical emission spectra collection system consisted of a spectroscope, fibre and related software. Optical emission spectroscopy (OES) was performed with a Maya2000 fibre optic spectrometer (Ocean Optics, Inc., Winter Park, FL). One end of the

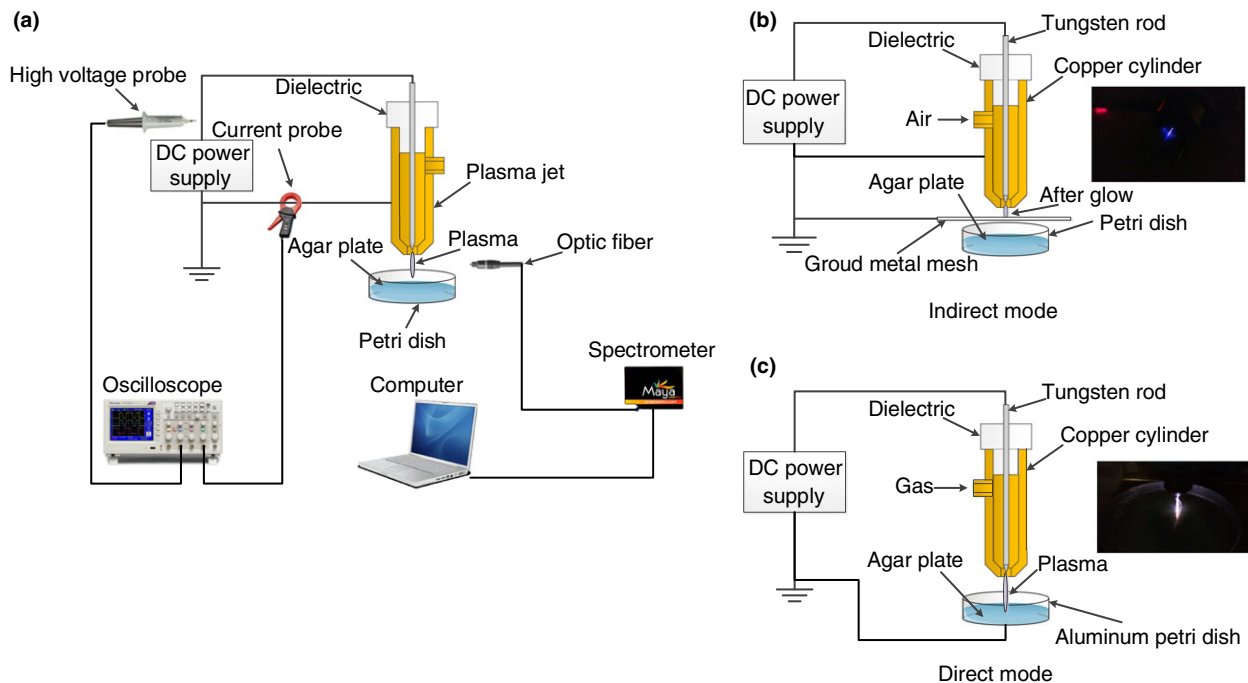


Figure 1 (a) Main components of the experimental setup. (b) Indirect mode of nonthermal plasma treatment. (c) Direct mode of nonthermal plasma treatment. [Colour figure can be viewed at wileyonlinelibrary.com].

fibre was placed near the nozzle of the plasma jet. The spectral data were analysed using SpectraSuit software (Ocean Optics, Inc.).

Plasma treatment

In this study, two modes of plasma treatment were tested, namely indirect mode for air or nitrogen plasma treatment and direct mode for argon plasma treatment (Fig. 1b). The agar plates were placed under the plasma jet to expose the bacteria to APNTP. In the indirect mode, the agar was not earthed. The distance between the bacteria and nozzle was approx. 15 mm for air plasma treatment and 9 mm for nitrogen treatment, while the flow rate of air was 1.5 l min⁻¹ and the flow rate of nitrogen was 8 l min⁻¹. Given the high flow rate of the flowing nitrogen gas and relatively small distance (9 mm), ambient air could not reach the bacteria. The air over the bacteria on the agar plate was edged out by the flowing nitrogen gas. The excited nitrogen and nitrogen ions were the only plasma agent that could reach *E. coli* on the agar plates. When air was used as the working gas, the bacteria were treated by air plasma with or without earth stainless steel woven wire mesh. The earth stainless steel woven wire mesh (0.5 mm wire diameter and 9 × 9 meshes per cm²) was placed between bacteria and plasma to separate the charged particles from the bacteria (Fig. 1b). Thus, the bactericidal effect of reactive species could be analysed without interference from charged particles. In the direct mode, the earth metal mesh was removed, and the agar plate was placed in the aluminium Petri dish. The agar in aluminium Petri dish was earthed by connecting aluminium Petri dish to ground (Fig. 1b). The distance between the bacteria and electrodes was approx. 9 mm, and the flow rate of argon was 8 l min⁻¹. Given the high flow rate, high density of the flowing argon gas and relatively small distance (9 mm), ambient air could not reach the bacteria. The air over the bacteria on the agar plate was edged out by the flowing argon gas. The excited argon and argon ions were the only plasma agent that could reach *E. coli* on the agar plates. *Escherichia coli* was treated with plasma (working gas: air) at 5.5 kV for 1.5, 2, 2.5, 3, 3.5 and 5.5 min or treated with plasma (working gas: argon) at 4.5 kV for 1, 1.5, 2, 2.5 and 6.5 min. *Escherichia coli* exposed to working gases (air or argon) only was used as control. To establish whether UV radiation plays a major role in the sterilization process, we placed a quartz glass plate JGS1 (Wuxi Crystal Optical Instrument, Jiangsu, China) above the bacteria in the indirect mode such that the bacterial sample was exposed to UV radiation alone. To analyse the role of UV radiation in the sterilization process, OES was performed over a wide wavelength range from 200 to 1100 nm in the direct mode.

Bacterial inoculation

The *E. coli* CICC 23796 used in this study was obtained from the China Center of Industrial Culture Collection. The stock culture was maintained at -80°C prior to use. *Escherichia coli* was inoculated brain heart infusion (Bacto, Sparks, MD) broth and incubated in a shaking incubator (HLD Laboratory Equipment Co., Jiangsu, China) for 24 h at 37°C and 200 rev min⁻¹. To determine bacterial concentration in the original culture, the culture was serially diluted with phosphate-buffered saline (PBS; Sigma Chemical Co., St Louis, MO) and inoculated onto Luria-Bertani (LB) agar plates for colony counts. Appropriate dilutions of the cultures were made to produce concentration of approx. 10³ CFU per ml. Sterile LB agar plates were subsequently inoculated with 0.1 ml of this dilution to yield 10² colonies per agar plate for colony count and plasma inactivation. Three identical replicate plates were prepared for each treatment.

Sample analysis

After the respective treatments, the bacterial cultures were incubated for 24 h until the colonies were large enough to be counted. The inactivation effect was quantified by calculating the log reduction factor (RF) as defined by Daeschlein *et al.* (2010).

$$\text{RF} = \log_{10}(\text{CFU controls}) - \log_{10}(\text{CFU after treatments}) \quad (1)$$

Given the differential inactivation effects, the treatment area was divided into three parts (Kolb *et al.* 2012). The immediate area under the nozzle of plasma jet in this study was a circle, which had a radius of 2.5 mm (the same as the nozzle's radius). Provided that the area of growth inhibition zone just exceeds the immediate area (Fig. 2), the plasma jet can inactivate the current concentration of the bacterial cultures. In this study, only the reduction in the number of colony-forming units in the immediate area was considered. The limits of the growth inhibition zone were not obvious when the bacterial concentration was lower than 10³ CFU per ml. Data for bacterial cultures with concentration lower than 10³ CFU per ml were not available, so the results of experiments involving those were not taken into account. The experiments were conducted in triplicate.

Microscope study

To further investigate the role of plasma in bacterial inactivation and the underlying mechanism, we employed

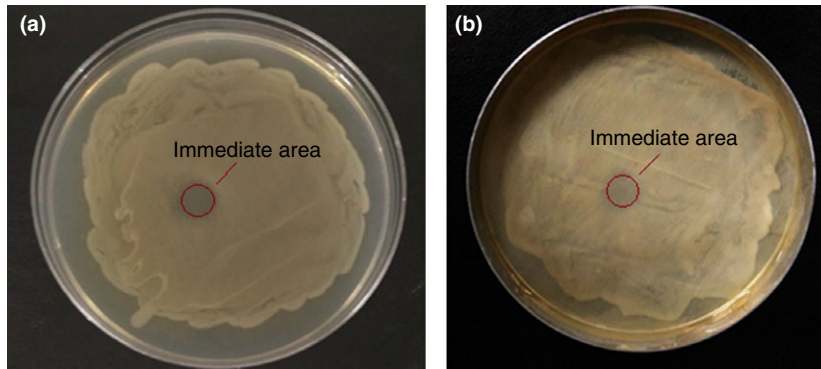


Figure 2 (a) Bystander effect where the area of growth inhibition zone exceeded the immediate area in the indirect mode. (b) Bystander effect where the area of growth inhibition zone exceeded the immediate area in the direct mode. [Colour figure can be viewed at wileyonlinelibrary.com].

scanning electron microscope (SEM), fluorescence microscopy and transmission electron microscope (TEM) imaging. After 24-h incubation, the colonies on the agar plate were exposed to APNTP. After plasma treatment, the colonies treated by plasma were stripped from the agar plate and then fixed in Karnovsky's fixative (2% v/v paraformaldehyde and 2% v/v glutaraldehyde in 1x PBS) overnight. The specimens were dehydrated using increasing concentrations of ethanol (30%, 50%, 70%, 80%, 90%, 95% and 100%). For SEM analysis, specimens were transferred to a mixture of alcohol and isoamyl acetate (50% v/v) for about 30 min and then transferred to pure isoamyl acetate for about 1 h or overnight. In the end, the specimens were dehydrated in Hitachi Model HCP-2 (Hitachi Koki, Tokyo, Japan) critical point drier with liquid carbon dioxide. In order to prevent surface charging by the electron beam, the samples were sputter-coated with gold particles using Sputter Coating Unit (Emitech K575X Quorum Emitech, Ashford, UK) resulting in a coating of 10 nm after 30 s. All observations were carried out with Hitachi SU8010 SEM (Hitachi High-Tech Manufacturing & Service, Corp., Tokyo, Japan). For TEM analysis, the specimens were placed in a 1 : 1 mixture of absolute acetone and the final spurr resin mixture for 1 h at room temperature, and then transferred to 1 : 3 mixture of absolute acetone and the final resin mixture for 3 h and to final spurr resin mixture overnight. Then, the specimens were placed in an Eppendorf tube containing spurr resin and heated at 70°C for more than 9 h. The specimens were sectioned using a LEICA EM UC7 ultratome, and the sections were stained with uranyl acetate and alkaline lead citrate for 5–10 min each and observed using a Hitachi Model H-7650 TEM (Hitachi High-Tech Manufacturing & Service, Corp.). For fluorescence imaging, the specimens treated by argon plasma were concentrated to 106 CFU per ml, stained with SYBR Green I (Invitrogen, Carlsbad, CA) under room temperature for 15 min in the dark and observed by fluorescence microscopy (Nikon Eclipse Ti-s, Tokyo, Japan). The experiments were performed in triplicate.

Statistical analysis

Three samples were collected for microbial counts in each experiment. The results were statistically analysed using the SAS 9.3 program (SAS Inst. Inc., Gary, NC). The surviving populations of *E. coli* after APNTP treatment were subjected to ANOVA. Means were compared according to Fisher's least significant difference method at the 0.05 level.

Results

Reduction in air and argon plasma-treated *Escherichia coli*

Bystander effect was observed where the area of growth inhibition zone exceeded the immediate area in the direct and indirect modes (Fig. 2). The log RFs for the direct and indirect modes are shown in Fig. 3. The results showed that 5.5 min of exposure to air plasma led to 8-log reduction in *E. coli*, whereas 6.5 min of exposure to

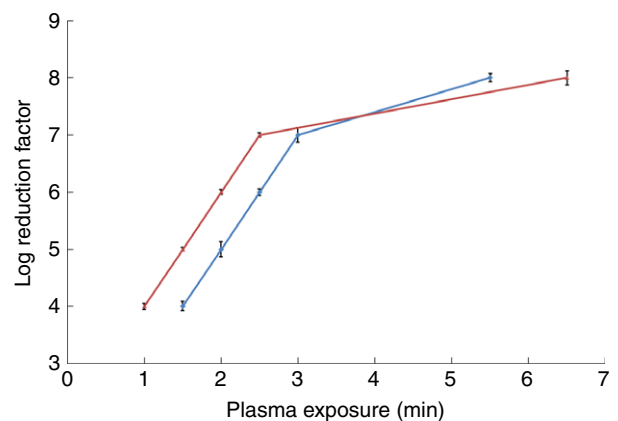


Figure 3 Reduction in air plasma-treated *Escherichia coli* (—◆—) at 5.5 kV and argon plasma-treated *E. coli* (—▲—) at 4.5 kV and 0.1 mA. [Colour figure can be viewed at wileyonlinelibrary.com].

argon plasma was required to achieve the same level of reduction.

Optical emission spectroscopy of argon and air nonthermal plasma

The OES of argon plasma under this experimental condition (4.5 kV and 0.1 mA) is shown in Fig. 4a. The emission spectra were dominated by excited Ar^* (738.4, 751.47, 763.51, 811.53 and 842.46 nm) and Ar^+ (418.96, 545.63 and 656.42 nm). The OES of the air plasma is also shown in Fig. 4b. Emissions were clearly observed at 315.9, 337.1, 353.7, 357.7 and 380.5 nm from the N_2 second positive system ($\text{C}^3\Pi_u-\text{B}^3\Pi_g$). N_2^+ emissions at 391.4 and 399.5 nm were also observed.

SEM, TEM and fluorescence microscopy observations

In Fig. 5, morphological changes and cell rupture were observed in *E. coli* after air plasma treatment. No obvious morphological changes were present in those treated with argon or nitrogen plasma treatment. As shown in Fig. 6,

most of the bacteria were intact in controls, the damage of bacteria increased over treatment time. In Fig. 6, fluorescence signals of the treated specimens were not significantly different from that of the controls.

Discussion

Assessment of the effects of various inactivation agents on nonthermal plasma

The temperatures of air and argon plasma were measured using a noncontact thermometer and found to be very close to the ambient temperature. Thus, the effect of temperature could be ignored. Bacterial DNA can be highly damaged by absorption of radiation at approx. 250 nm, which leads to rapid cell death (Lindberg and Horneck 1991; Lerouge *et al.* 2000; Philip *et al.* 2002; Boudam and Moisan 2010). As shown in Fig. 4, doses of 200–300 nm UV radiation were too low for air and argon plasma. By contrast, no bactericidal effect was observed with quartz glass plates (data not shown). The bactericidal effect of UV radiation could be ignored in the air or argon plasma

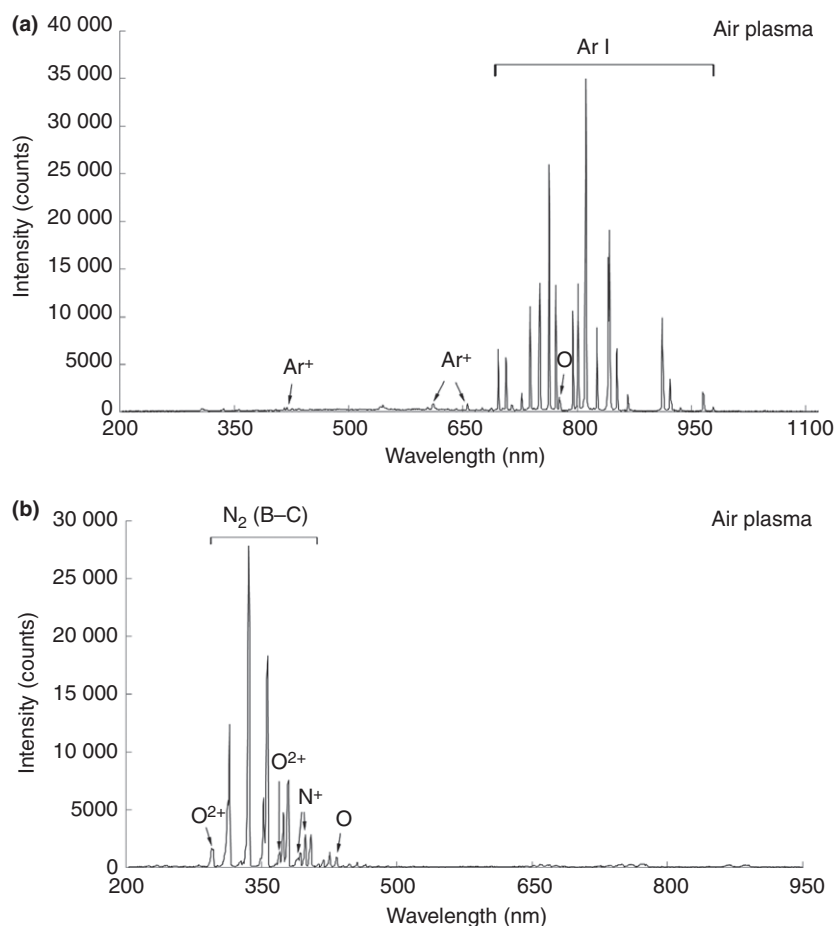


Figure 4 (a) Optical emission spectroscopy of argon nonthermal plasma at 4.5 kV and 0.1 mA. (b) Optical emission spectroscopy of air nonthermal plasma at 5.5 kV.

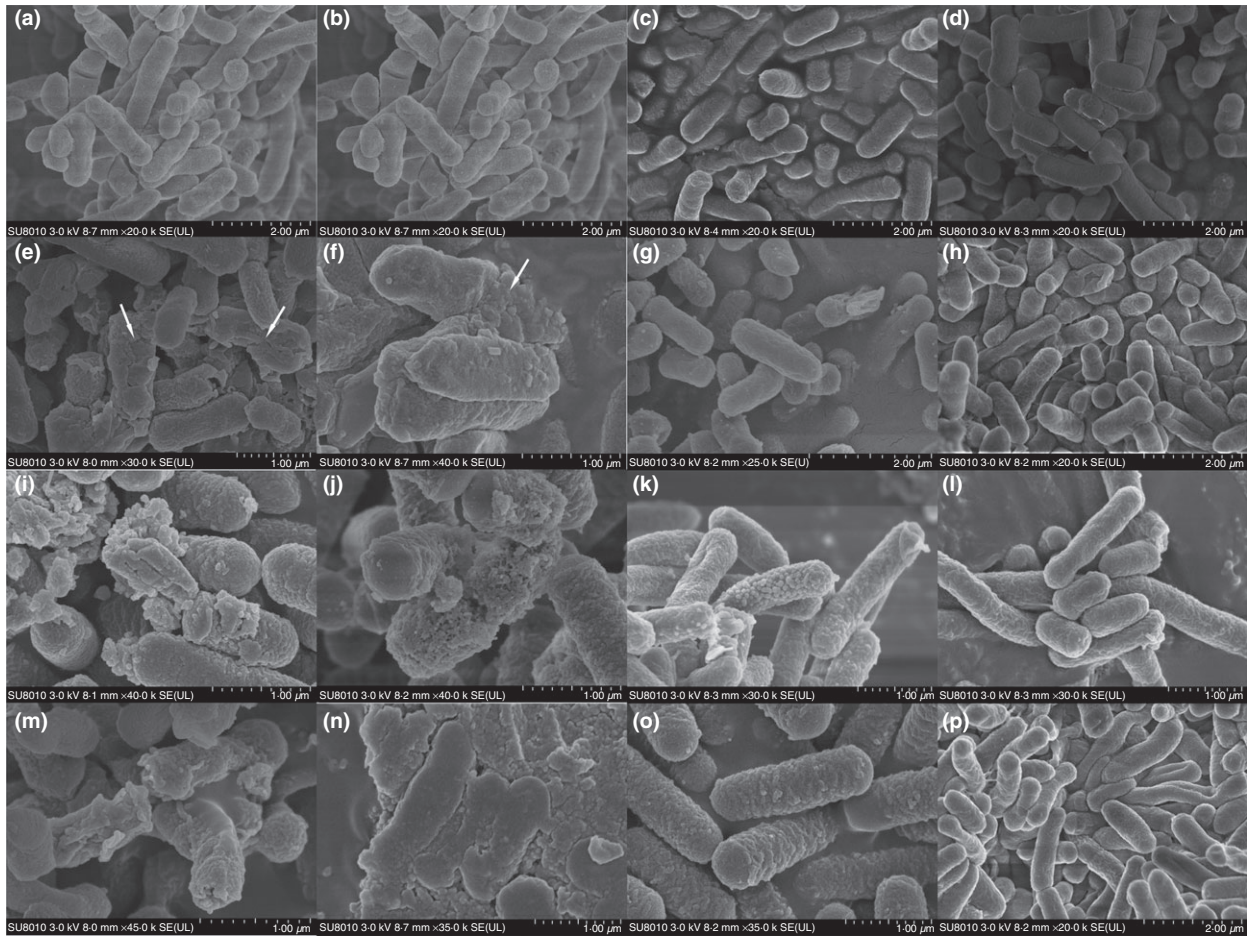


Figure 5 (a, b) Scanning electron microscopic (SEM) images of control samples of air plasma treatment (with or without earth metal mesh). (c) SEM image of control sample of argon plasma treatment. (d) SEM image of control samples of pure nitrogen plasma treatment. SEM image of air plasma-treated sample with earth metal mesh at 5.5 kV and either 5 (e), 3 (i) or 1 (m) min of exposure. SEM image of air plasma-treated sample without earth metal mesh at 5.5 kV and either 5 (f), 3 (j) or 1 (n) min of exposure. SEM image of argon plasma-treated sample at 4.5 kV and 0.1 mA and either 5 (g), 3 (k) or 1 (o) min of exposure. SEM image of pure nitrogen plasma-treated sample at 4.5 kV and either 5 (h), 3 (l) or 1 (p) min of exposure. The white arrows indicate the cell rupture of *Escherichia coli*.

treatment systems. Therefore, temperature and UV radiation did not play a major role in the inactivation of bacteria in this study. The experimental results in the control groups showed that applied air or argon gas did not reduce *E. coli* growth, suggesting the absence of detectable bacterial inactivation caused by applied air or argon flow (data not shown). Consequently, the inactivation effect was only caused by agents generated by non-thermal plasma. The OES of argon plasma under this experimental condition is shown in Fig. 4a. This result indicated that only Ar^* and Ar^+ existed in the core of the discharge region, and the flow rate could prevent ambient air from coming into contact with bacteria in the direct mode. Consequently, the physical inactivation mechanism of charged particles proposed by Mendis *et al.* (2000) could be studied without the interference of reactive

species. Weak O radical emission at 777.2 nm was also observed, which may be attributed to discharge at the pure argon–ambient air interface.

To inspect the bactericidal effect of the excited nitrogen molecule in the indirect mode, pure nitrogen gas was used as the working gas to generate nitrogen plasma. The flow rate of pure nitrogen gas was very high and the distance between the nozzle and bacteria was small (9 mm, same as the direct mode) to edge out the air over the sample. Thus, only nitrogen, excited N_2^* and N_2^+ were in contact with the bacteria. The experimental results showed that the bactericidal effect of the excited nitrogen molecule was limited, with lower than 4-log reduction after 5 min of treatment. The excited N_2^* and N_2^+ were not expected to play significant roles in the inactivation of air plasma treatment. Therefore, the high sterilization

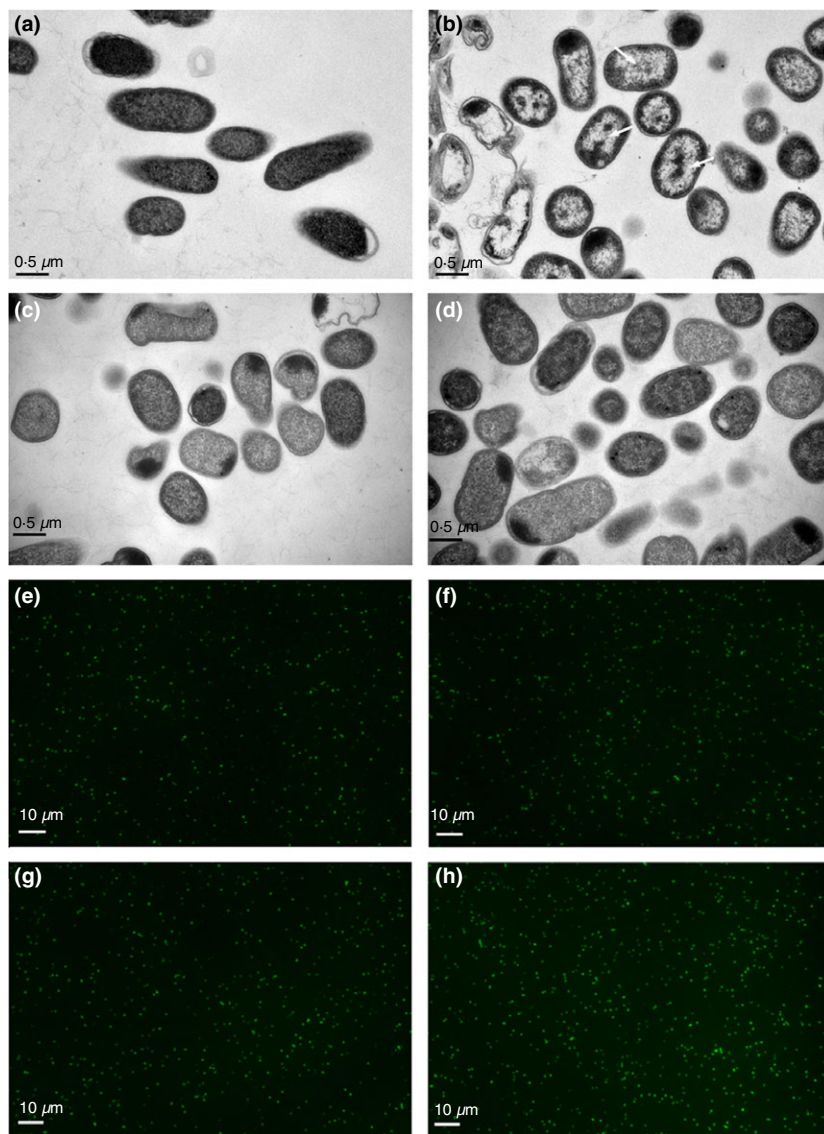
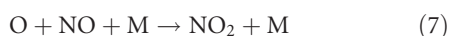
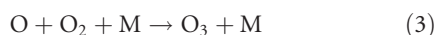
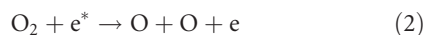


Figure 6 (a) Transmission electron microscopic (TEM) image of control. TEM images of argon plasma-treated sample at 4.5 kV, 0.1 mA and either 6 (b), 4 (c) or 2 (d) min of exposure. (e) Fluorescence microscopy image of the control sample. Fluorescence microscopy images of argon plasma-treated sample at 4.5 kV, 0.1 mA and either 6 (f), 4 (g) or 2 (h) min of exposure. The white arrows indicate the leakage of the cytoplasmic contents of *Escherichia coli*. [Colour figure can be viewed at wileyonlinelibrary.com].

efficiency was mainly attributed to oxygen radicals, ozone and nitrogen oxide. The formation of oxygen radicals and nitrogen oxide can be described by the following reactions (Eliasson *et al.* 1987; Hill and Smoot 2000; Ahn *et al.* 2003; Deng *et al.* 2013):



where $\text{M}=\text{O}$, O_2 or O_3 , a third collision partner. Based on the experimental results, elemental oxygen played an essential role in inducing the reactive species to influence

an interaction with the micro-organism (Guo *et al.* 2015). The life span of singlet oxygen in a gaseous atmosphere is relatively short, in the order of milliseconds (Khalil *et al.* 2005). Nevertheless, the O atoms could react with water molecules in the air, thereby resulting in the formation of OH radicals (Yusupov *et al.* 2014). Therefore, the reactive species generated by the atomic oxygen could be expected to directly act on the bacteria. The ozone, OH radicals, and nitrogen oxide probably play major roles in the inactivation of air plasma treatment.

Charged particles and reactive species in the inactivation mechanism

As shown in Fig. 5, morphological changes and cell rupture were observed in *E. coli* after air plasma treatment,

whereas no obvious morphological changes were present in those treated with argon plasma treatment. When the agar plate was not earthed (using a common Petri dish) in the argon plasma treatment condition, the discharge current was nearly zero and very limited bactericidal effect was observed, even though the voltage (9 kV) was much higher than that in the case of agar plate being earthed (data not shown). When the agar plate was earthed (using a metal Petri dish) and the discharge current reached 0.1 mA, 8-log reduction of *E. coli* was achieved after 6.5 min argon plasma treatment in the direct mode.

When the agar plate is not earthed, few free charges are available for transfer under a discharge current of almost zero, and the charged particles can accumulate outside the bacterial surface. The accumulated electric charge causes electrostatic stress that is sufficient to exceed the membrane's material tensile strength in an alternating current dielectric barrier discharge plasma system (Laroussi *et al.* 1999; Mendis *et al.* 2000). However, in this study, we did not observe any disruption of the cell structure in the direct mode (Fig. 5 g,k,o), whereas no bactericidal effect was observed when the discharge current was almost zero. Given that argon ions could reach the bacteria, we conclude that the physical mechanism proposed by Mendis *et al.* is unlikely to explain the observations made using a DC plasma system.

The bactericidal effect was obvious when the discharge current reached 0.1 mA. However, we did not observe any disruption of cell structure under this experimental condition (4.5 kV, 5 min treatment time, 8 l min⁻¹ working gas flow rate, and 9 mm distance), as shown in Fig. 5 g,k,o. The possibility of internal damage could not be excluded, so we used TEM imaging to detect possible changes inside the bacteria. Compared with the controls, cytoplasmic contents inside these bacteria were not uniform in appearance. In fact, the colours of their cytoplasmic structures suggested that these bacteria may have lower cytoplasmic contents compared with controls (Fig. 6a). This trend was likely caused by change in membrane permeability and cell membrane damage, which resulted in leakage of the cytoplasmic contents and bacterial death. Fluorescence imaging was employed to detect whether DNA inside the cells was destroyed by the plasma. However, we found that fluorescence signal of the treated specimens was not significantly different from that of the controls (Fig. 6e). This result indicated that argon plasma did not destroy the DNA of the treated specimens in the direct mode.

In the indirect mode (air plasma treatment), the charged particles were unable to reach the bacteria on the agar plate because of the earth metal mesh. As seen in Fig. 5e,f,i,j,m,n, no significant differences were

observed when the earth metal mesh was used or not used in the indirect mode. The bactericidal effect and morphological changes of *E. coli* in the indirect mode were mainly caused by reactive species (Timoshkin *et al.* 2012; Li *et al.* 2013). As shown in Fig. 5e,f,i,j,m,n, the cell walls were completely ruptured after air plasma treatment. However, neither obvious morphological changes nor rupture of the cell wall were observed in *E. coli* after pure nitrogen plasma treatment (Fig. 5h,l,p). These results suggested that oxidative stress was the likely mechanism behind the inactivation caused by the reactive species. Yusupov *et al.* (2013) investigated the interaction of important plasma species with bacterial peptidoglycan by reactive molecular dynamics simulation. Their results showed that OH radicals and ozone could destroy bacterial cell walls by breaking important bonds in peptidoglycan, such as the C–O, C–N and C–C bonds (Yusupov *et al.* 2013). Likewise, breakage of important peptidoglycan bonds via strong oxidative stress caused by OH radicals, ozone and nitrogen oxide may also account for the disruption of bacterial cell wall and membrane in our study. Thus, this mechanism likely underlies the effects observed upon interaction of reactive species with bacteria in indirect mode of a DC nonthermal plasma treatment system.

Data presented in this study demonstrated that elemental oxygen played an essential role in the induction of reactive species to influence interaction with microorganisms. While N₂⁺ and N₂⁺ are not expected to play a significant role, ozone, OH radicals and nitrogen oxide likely play major roles in the inactivation of bacteria by air plasma treatment. Results of our argon plasma treatment experiments showed that electrostatic disruption of bacteria by charged particle accumulation may not be the mechanism by which bacteria are inactivated in a DC nonthermal plasma treatment system. However, the results of the air plasma treatment experiments showed that oxidative stress caused by ozone, OH radicals and nitrogen oxide on peptidoglycans and lipids in the cell wall and membrane underlie the mechanism behind inactivation of bacteria by air plasma.

Acknowledgements

The authors gratefully acknowledge the financial support provided by the National Natural Science Foundation of China (31271613/C130102) and the China Postdoctoral Science Foundation (2014M551748).

Conflict of Interest

No conflict of interest declared.

References

- Ahn, H.S., Hayashi, N., Ihara, S. and Yamabe, C. (2003) Ozone generation characteristics by superimposed discharge in oxygen-fed ozonizer. *Jpn J Appl Phys* **42**, 6578–6583.
- Baier, M., Foerster, J., Schnabel, U., Knorr, D., Ehlbeck, J., Herppich, W.B. and Schlueter, O. (2013) Direct non-thermal plasma treatment for the sanitation of fresh corn salad leaves: evaluation of physical and physiological effects and antimicrobial efficacy. *Postharvest Biol Technol* **84**, 81–87.
- Bermudez-Aguirre, D., Wemlinger, E., Pedrow, P., Barbosa-Canovas, G. and Garcia-Perez, M. (2013) Effect of atmospheric pressure cold plasma (APCP) on the inactivation of *Escherichia coli* in fresh produce. *Food Control* **34**, 149–157.
- Boudam, M.K. and Moisan, M. (2010) Synergy effect of heat and UV photons on bacterial-spore inactivation in an N₂-O₂ plasma-afterglow sterilizer. *J Phys D-Appl Phys* **43**, 295202.
- Daeschlein, G., von-Woedtke, T., Kindel, E., Brandenburg, R., Weltmann, K.D. and Jünger, M. (2010) Antibacterial activity of an atmospheric pressure plasma jet against relevant wound pathogens in vitro on a simulated wound environment. *Plasma Process Polym* **7**, 224–230.
- Deng, X.T., Shi, J.J. and Kong, M.G. (2006) Physical mechanisms of inactivation of *Bacillus subtilis* spores using cold atmospheric plasmas. *IEEE Trans Plasma Sci* **34**, 1310–1316.
- Deng, X.L., Yu, A., Nikiforov, P., Vanraes, P. and Leys, C. (2013) Direct current plasma jet at atmospheric pressure operating in nitrogen and air. *J Appl Phys* **113**, 023305.
- Digel, I., Artmann, A.T., Nishikawa, K., Cook, M., Kurulgan, E. and Artmann, G.M. (2005) Bactericidal effects of plasma-generated cluster ions. *Med Biol Eng Comput* **43**, 800–807.
- Eliasson, B., Hirth, M. and Kogelschatz, U. (1987) Ozone synthesis from oxygen in dielectric barrier discharges. *J Phys D-Appl Phys* **20**, 1421–1437.
- Fernandez, A., Noriega, E. and Thompson, A. (2013) Inactivation of *Salmonella enterica* serovar Typhimurium on fresh produce by cold atmospheric gas plasma technology. *Food Microbiol* **33**, 24–29.
- Fletcher, L.A., Gaunt, L.F., Beggs, C.B., Shepherd, S.J., Sleight, P.A., Noakes, C.J. and Kerr, K.G. (2007) Bactericidal action of positive and negative ions in air. *BMC Microbiol* **7**, 32.
- Guo, J., Huang, K. and Wang, J. (2015) Bactericidal effect of various non-thermal plasma agents and the influence of experimental conditions in microbial inactivation: a review. *Food Control* **50**, 482–490.
- Hill, S.C. and Smoot, L.D. (2000) Modeling of nitrogen oxides formation and destruction in combustion systems. *Prog Energy Combust Sci* **26**, 417–458.
- Jahid, I.K., Han, N. and Ha, S.D. (2014) Inactivation kinetics of cold oxygen plasma depend on incubation conditions of *Aeromonas hydrophila* biofilm on lettuce. *Food Res Int* **55**, 181–190.
- Jahid, I.K., Han, N., Zhang, C.Y. and Ha, S.D. (2015) Mixed culture biofilms of *Salmonella* Typhimurium and cultivable indigenous microorganisms on lettuce show enhanced resistance of their sessile cells to cold oxygen plasma. *Food Microbiol* **46**, 383–394.
- Khalil, G., Chang, A., Gouterman, M., Callis, J.B., Dalton, L., Turro, N. and Jockusch, S. (2005) Oxygen pressure measurement using singlet oxygen emission. *Rev Sci Instrum* **76**, 054101.
- Kolb, J.F., Mattson, A.M., Edelblute, C.M., Hao, X.L., Malik, M.A. and Heller, L.C. (2012) Cold dc-operated air plasma jet for the inactivation of infectious microorganisms. *IEEE Trans Plasma Sci* **40**, 3007–3026.
- Lacombe, A., Niemira, B.A., Gurtler, J.B., Fan, X.T., Sites, J., Boyd, G. and Chen, H.Q. (2015) Atmospheric cold plasma inactivation of aerobic microorganisms on blueberries and effects on quality attributes. *Food Microbiol* **46**, 479–484.
- Laroussi, M., Saylor, G.S., Glascock, B.B., McCurdy, B., Pearce, M.E., Bright, N.G. and Malott, C.M. (1999) Images of biological samples undergoing sterilization by a glow discharge at atmospheric pressure. *IEEE Trans Plasma Sci* **27**, 34–35.
- Lee, H., Kim, J.E., Chung, M.S. and Min, S.C. (2015) Cold plasma treatment for the microbiological safety of cabbage, lettuce, and dried figs. *Food Microbiol* **51**, 74–80.
- Lerouge, S., Fozza, A.C., Wertheimer, M.R., Marchand, R. and Yahia, L.H. (2000) Sterilization by low-pressure plasma: the role of vacuum-ultraviolet radiation. *Plasma Process Polym* **5**, 31–46.
- Li, J., Sakai, N., Watanabe, M., Hotta, E. and Wachi, M. (2013) Study on plasma agent effect of a direct-current atmospheric pressure oxygen-plasma jet on inactivation of *E. coli* using bacterial mutants. *IEEE Trans Plasma Sci* **41**, 935–941.
- Lindberg, C. and Horneck, G. (1991) Action spectra for survival and spore photoproduct formation of *Bacillus subtilis* irradiated with short-wavelength (200–300 nm) UV at atmospheric pressure and in vacuo. *J Photochem Photobiol B-Biol* **11**, 69–80.
- Mendis, D.A., Rosenberg, M. and Azam, F. (2000) A note on the possible electrostatic disruption of bacteria. *IEEE Trans Plasma Sci* **28**, 1304–1306.
- Misra, N.N., Patil, S., Moiseev, T., Bourke, P., Mosnier, J.P., Keener, K.M. and Cullen, P.J. (2014) In-package atmospheric pressure cold plasma treatment of strawberries. *J Food Eng* **125**, 131–138.
- Pankaj, S.K., Bueno-Ferrer, C., Misra, N.N., Milosavljevic, V., O'Donnell, C.P., Bourke, P., Keener, K.M. and Cullen, P.J. (2014) Applications of cold plasma technology in food packaging. *Trends Food Sci Technol* **35**, 15–17.

- Philip, N., Saoudi, B., Crevier, M.C., Moisan, M., Barbeau, J. and Pelletier, J. (2002) The respective roles of UV photons and oxygen atoms in plasma sterilization at reduced gas pressure: the case of N₂-O₂ mixtures. *IEEE Trans Plasma Sci* **30**, 1429–1436.
- Pompl, R., Jamitzky, F., Shimizu, T., Steffes, B., Bunk, W., Schmidt, H.U., Georgi, M., Ramrath, K. et al. (2009) The effect of low-temperature plasma on bacteria as observed by repeated AFM imaging. *New J Phys* **11**, 11.
- Pradeep, P. and Chulkyoon, M. (2016) Non-thermal plasmas (NTPs) for inactivation of viruses in abiotic environment. *Res J Biotechnol* **11**, 91–96.
- Suhem, K., Matan, N., Nisoa, M. and Matan, N. (2013) Inhibition of *Aspergillus flavus* on agar media and brown rice cereal bars using cold atmospheric plasma treatment. *Int J Food Microbiol* **161**, 107–111.
- Timoshkin, I.V., Maclean, M., Wilson, M.P., Given, M.J., MacGregor, S.J., Wang, T. and Anderson, J.G. (2012) Bactericidal effect of corona discharges in atmospheric air. *IEEE Trans Plasma Sci* **40**, 2322–2333.
- Yusupov, M., Bogaert, A., Huygh, S., Snoeckx, R., van-Duin, A.C.T. and Neyts, E.C. (2013) Plasma-induced destruction of bacterial cell wall components: as reactive molecular dynamics simulation. *J Phys Chem C* **117**, 5993–5998.
- Yusupov, M., Neyts, E.C., Simon, P., Berdiyrov, G., Snoeckx, R., van-Duin, A.C.T. and Bogaerts, A. (2014) Reactive molecular dynamics simulations of oxygen species in a liquid water layer of interest for plasma medicine. *J Phys D-Appl Phys* **47**, 025205.
- Ziuzina, D., Han, L., Cullen, P.J. and Bourke, P. (2015) Cold plasma inactivation of internalised bacteria and biofilms for *Salmonella enterica serovar* Typhimurium, *Listeria monocytogenes* and *Escherichia coli*. *Int J Food Microbiol* **210**, 53–61.